

STM studies of thin PTCDA films on Ag/Si(111)- $\sqrt{3}\times\sqrt{3}$

J. B. Gustafsson,* H. M. Zhang, and L. S. O. Johansson

Department of Physics, Karlstad University, SE-651 88 Karlstad, Sweden

(Received 2 March 2006; revised manuscript received 26 February 2007; published 16 April 2007)

Thin films of the large planar organic molecule 3,4,9,10-perylene tetracarboxylic dianhydride on the Ag/Si(111)- $\sqrt{3}\times\sqrt{3}$ surface have been studied by scanning tunneling microscopy. The coverage was between 0.3 and 10 monolayers. In submonolayers the molecules form two different phases with a commensurate relationship to the substrate: a herringbone phase and a square phase. Adsorption sites are determined for the square phase. Additional herringbone phases were also observed with other unit cell size or lower order in relation to the substrate. The molecules lie flat on the surface and form a full monolayer before multilayers are developed. Both the square and herringbone phases have been observed for the second layer. With more than 3 layers, islands were built up layer by layer in agreement with the α bulk phase. On top of the islands there was always a herringbone structure.

DOI: 10.1103/PhysRevB.75.155414

PACS number(s): 68.37.Ef

I. INTRODUCTION

Organic molecules can be tailored with a rich variation of functionalities. In order to exploit this in devices like organic light-emitting diodes and field-effect transistors, the interface properties of the organic materials and various substrates need a good understanding. For this purpose the planar perylene derivative 3,4,9,10-perylene tetracarboxylic dianhydride (PTCDA) has been widely used as a model material in studies of the growth and electronic properties of semiconducting organic thin films. The ordering of this type of large molecules is usually dependent on a combination of the interaction between molecules, molecule substrate, and also the lattice parameters of the substrate. Additional factors can be growth speed and substrate temperature.^{1,2}

Well-ordered films of flat-lying PTCDA molecules can be formed on weakly interacting surfaces like Au³ and highly oriented pyrolytic graphite (HOPG).⁴ A reactive semiconductor surface often gives a more disordered structure of the film due to the substrate dangling bonds^{5,6} and a passivation of the substrate often enhances the film quality. For surfaces with intermediate interaction strength, true epitaxial growth with site recognition can be found. One prominent example is Ag where the PTCDA molecules on the Ag(111) surface form a herringbone structure with two molecules per unit cell,^{1,7,8} while on the Ag(110) surface they form a nearly square phase with one molecule per unit cell³ in a brick wall ordering. On Au(111) and Au(100) a squarelike unit cell is reported simultaneously with a herringbone phase.⁹ In all these cases a commensurate relationship between the molecules and the substrate is reported. For semiconductor substrates the ordering is usually attributed to a point on the line relationship with the substrate, or in cases where the dangling bonds of a semiconductor surface interact strongly with the molecules, a disordered first layer is seen.^{10,11}

We have studied PTCDA growth on the Ag/Si(111)- $\sqrt{3}\times\sqrt{3}$ surface which is a semi conducting surface.¹² The structure of the surface has been described with the so-called honeycomb-chain-trimer (HCT) model¹² at room temperature with the atomic structure shown in Fig. 1(a). At low temperature, an asymmetry in the Ag triangles of the unit cell

has been observed by scanning tunneling microscopy (STM),¹³ which resulted in the proposal of the inequivalent triangle (IET) model, in which the Ag atoms are slightly displaced compared to the HCT model. Recently, the IET structure was observed also at room temperature¹⁴ but for simplicity we choose to show the HCT model in Fig. 1. The surface-molecule interaction strength of the Ag/Si(111)- $\sqrt{3}\times\sqrt{3}$ surface could be expected to be in between the clean and passivated Si surfaces.

This surface has shown to be an excellent substrate for ordered submonolayer growth of large molecules like pentacene,¹⁵ C₆₀,^{16,17} phthalocyanines,¹⁸ endohedral

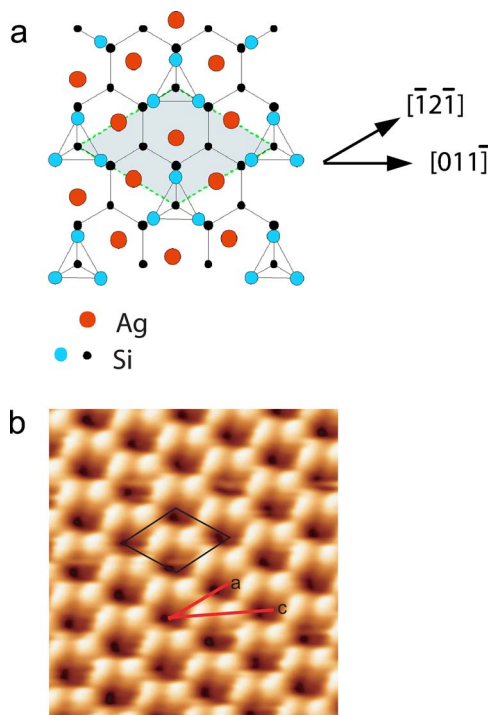


FIG. 1. (Color online) (a) Schematic atomic structure of the HCT model with the unit cell. The large circles are Ag. (b) Empty-state STM image of the clean Ag/Si(111)- $\sqrt{3}\times\sqrt{3}$ surface. Image size is $40\times 40 \text{ \AA}^2$, $V = +1.2 \text{ V}$, $I = 0.1 \text{ nA}$.

fullerenes,¹⁹ and NTCDI²⁰ as well as for hydrogen-bonded networks.²¹ Previous x-ray photoelectron spectroscopy (XPS) studies²² of PTCDA on Ag/Si(111)- $\sqrt{3} \times \sqrt{3}$ found an interaction between the PTCDA molecules and the substrate. Low-energy electron diffraction (LEED) images clearly showed ordered growth. The interaction was seen in new C 1s and O 1s core-level components. A very recent low-coverage [0.1 monolayer (ML)] STM study²³ of PTCDA on Ag/Si(111)- $\sqrt{3} \times \sqrt{3}$ showed that the herringbone, square, and a new hexagonal phase, with ordering in between the square and the herringbone phases, coexisted on the surface.

In this paper, PTCDA films ranging from submonolayers up to 10 ML have been characterized. The Ag/Si(111)- $\sqrt{3} \times \sqrt{3}$ surface was well suited for ordered growth in the first monolayer. We observed two different commensurate phases—a square phase and a herringbone phase—on Ag/Si(111)- $\sqrt{3} \times \sqrt{3}$. The herringbone phase was seen with two different unit cell sizes where the larger was identified as the one having a commensurate relation with the substrate. In the square phase adsorption sites have been determined. This phase was also found in the second layer but was not observed for thick bulklike films.

II. EXPERIMENTAL DETAILS

This study was done in ultrahigh vacuum (UHV) with a variable-temperature STM from Omicron Nanotechnology GmbH, equipped with separate analysis and preparation chambers. The tip was made from W/Ir, and all the voltages given in the paper were sample biased. The base pressures were 4×10^{-11} mbar in the preparation chamber and 8×10^{-11} mbar in the analysis chamber.

A Shiraki-etched²⁴ Sb-doped Si(111) sample cut from a wafer (Virginia Semiconductors Inc.), with a resistivity of 1–10 Ω cm, was used as substrate. It was outgassed *in situ* by resistive heating, slowly increasing the temperature to 600 °C for several hours. The substrate was cleaned by a stepwise increase of the temperature to 940 °C to remove the oxide. During cleaning the pressure was kept below 5×10^{-10} mbar.

The Si(111) sample showed a good 7×7 LEED reconstruction with sharp spots and low background. The surface was subsequently cleaned again by heating to 940 °C for 30 s. Then 3 Å of Ag was deposited as monitored by a quartz crystal microbalance. Subsequent annealing to 600 °C formed a $\sqrt{3} \times \sqrt{3}$ reconstruction with a sharp LEED pattern. Reference scans with STM showed a good quality $\sqrt{3} \times \sqrt{3}$ surface with domain sizes of about 50–100 nm.

PTCDA was deposited from a home built source, consisting of a crucible heated by a filament, while the sample was kept at room temperature. The source was out-gassed for several hours at temperature slightly below the deposition temperature. The deposition rate was calibrated with a quartz crystal microbalance and kept at about 0.4 Å/min. The pressure during deposition was 2×10^{-10} mbar.

III. RESULTS

The growth of PTCDA was done in several stages. We start with some initial remarks about the substrate and then

present results and discuss the ordering of molecules and film formation for each of the cases: submonolayer, complete monolayer, and thicker layers.

A. Ag/Si(111)- $\sqrt{3} \times \sqrt{3}$

Silver deposited on Si(111) forms a $\sqrt{3} \times \sqrt{3}$ reconstruction if the surface is annealed to a temperature about 550–600 °C for typically a few minutes, resulting in large nearly defect-free domains of the reconstructed surface. Figure 1 shows the HCT atomic structure model for Ag/Si(111)- $\sqrt{3} \times \sqrt{3}$ together with a high-resolution empty-state STM image.

The image has hexagonal features in a honeycomb structure related to the higher empty-state density at the center of the Ag trimers.¹³ The darker areas are connected to the Si trimers. Two principal high-symmetry directions are indicated by two vectors **a** $[\bar{1}2\bar{1}]$ and **c** $[01\bar{1}]$ in Fig. 1(b) and will be used when the molecular ordering is discussed. **a** has a length of 6.65 Å, which is $\sqrt{3}$ times the Si(111) 1×1 surface lattice 3.84 Å, and **c** is $3 \times 3.84 = 11.52$ Å. The surface unit cell has a threefold rotational symmetry in each domain. With a proper calibration to thermal drifts and piezocreeeping, unit cell sizes between 6.6 and 7.1 Å were obtained in the STM images. At the step edges a larger concentration of defects were observed. The defects are most likely related to some excess of Si atoms.

B. Submonolayer coverage

At 0.3 ML coverage the PTCDA molecules appear to be quite mobile on the surface after the deposition, as no single free molecule or smaller islands of just a few molecules were observed on the large terraces. A typical molecular island or domain together with a well-resolved substrate can be seen in Fig. 2. The molecules grow mainly in a well-ordered, relatively large, flat layer structure, preferably positioned next to a defect or a step edge. Regions of disorder were observed at some step edges. In such areas, high-resolution STM images of PTCDA molecules could not be obtained. Depending on the condition of the tip and the measuring parameters, the molecules can have different appearance and only in some cases detailed submolecular resolution was achieved.

As discussed above, the structure of the Ag/Si(111)- $\sqrt{3} \times \sqrt{3}$ surface is well known. This gives a very accurate reference of calibration on images with both ordered molecules and atomic resolution of the substrate. For areas where only the molecules can be seen there is generally a larger uncertainty about the distances and angles due to thermal drift and piezocreeeping. Two major molecular phases have been observed in the submonolayer range. The first one is a square phase with a nearly quadratic unit cell consisting of two molecules rotated 90° to each other, and the second one is a herringbone phase, shown in Fig. 2.

The square phase is similar to an ordering reported under some conditions for PTCDA on Au(111) and Au(100).⁹ The square-phase unit cell size with two molecules was measured as 16.2×16.2 Å² which gives an area of 262.4 Å². This area

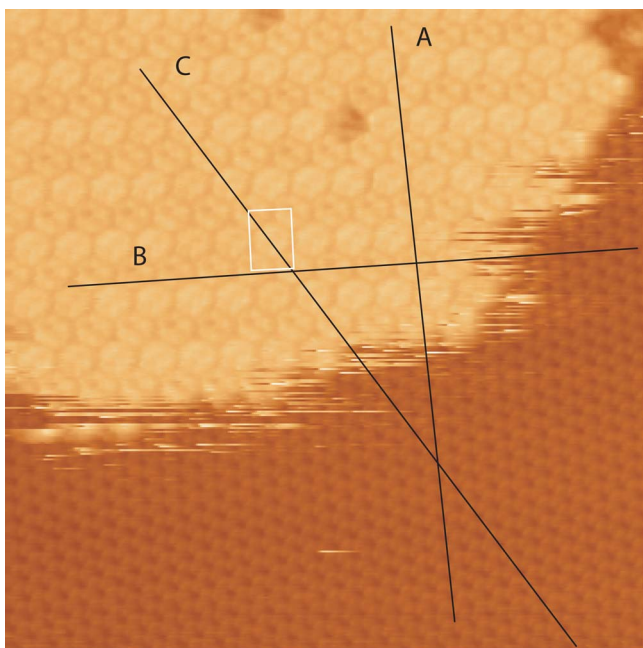


FIG. 2. (Color online) Molecular island at 0.3 ML coverage of PTCDA. The herringbone unit cell is shown. The two lines A and B are aligned with high-symmetry directions of the substrate. Note that the unit cell axis is slightly misaligned with these two directions. The line C in the diagonal direction is in the high-symmetry direction $[10\bar{1}]$. Tunnelling conditions: $V=+2.0$ V, $I=0.5$ nA. The image size is $230 \times 230 \text{ \AA}^2$.

is slightly larger than the PTCDA bulk phases that has an area close to 240 \AA^2 for both the α and β polymorph.⁴ The ordering of the molecules and the adsorption sites in the square phase can be related to the substrate reconstruction in Fig. 3 which shows a well-resolved image of both molecules and the substrate. Two equal-sized rectangles marked next to each other have each corner above a Si trimer. This shows that the centers of the molecules coinciding with the left side corners also have their adsorption sites on top of the Si trimers.

Measurements calibrated from the substrate and the contrast variations in STM images show that the smallest rectangular unit cell of the molecules where both the $\sqrt{3} \times \sqrt{3}$ substrate and molecular lattice points match is $6 \times 24\sqrt{3}$ relative to the 1×1 lattice of the Si(111) surface. This gives an area of $23.04 \times 159.6 \text{ \AA}^2$ with 28 molecules in the unit cell. Our measurements of the square phase are in agreement with

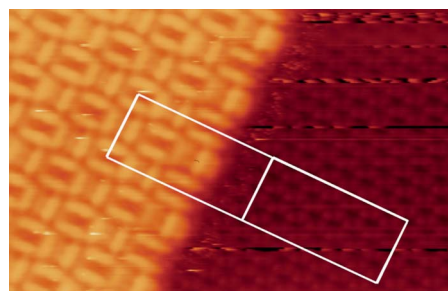


FIG. 3. (Color online) Adsorption points of the square phase. The two equal-sized rectangles have a Si trimer position in each corner. The two corners to the far left coincide with the center of a molecule and show molecular adsorption sites centered above a Si trimer. Image size $140 \times 90 \text{ \AA}^2$. $V=+0.806$ V, $I=0.196$ nA.

the recently reported results by Swarbrick *et al.*, where two different, higher-order commensurate square phases were proposed.²³ The intermolecular contrast and measurements calibrated to the substrate show that the square model with the dotted lines in Fig. 4(a) is in better agreement with our results and is also identical to the model reported by Swarbrick *et al.*²³ with the larger unit cell. We do not have any observation that clearly suggests a square model with a smaller unit cell.

By the geometry of the substrate and the square phase, the adsorption sites can be determined and are shown in Fig. 4. The smallest unit cell of this phase can be constructed by considering the molecules at the centers of each side that have the same adsorption sites. By connecting these points a diamond-shaped unit cell is formed, which is also shown in Fig. 4. Its matrix notation is given in Table I. There are seven different adsorption sites for each orientation of the molecules. It can be noted that the molecules with the same orientation as the ones in the corners of the rectangle have relatively similar contrast in the STM images while the molecules with same orientation as the one at the center of the short axis have a large contrast variation. The diamond-shaped unit cell is shown for a molecular layer in Figs. 4(b) and 5 where the repeating contrast variations are clearly seen. However, the position of the diamond-shaped unit cell with respect to the substrate may not coincide with the model in Fig. 4(a), since the substrate and molecular contrast variations could not be imaged simultaneously.

The herringbone phase is known from PTCDA growth on surfaces where the interaction with the substrate is small. The unit cell is rectangular with two molecules in each cell.

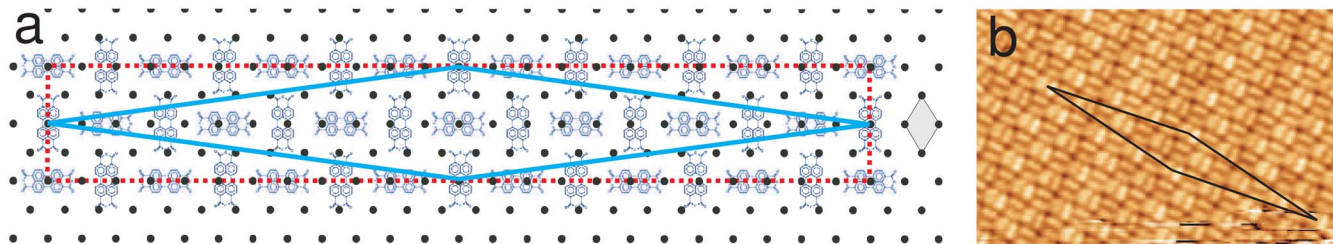


FIG. 4. (Color online) (a) The square model with the molecular positions in the unit cell. The substrate unit cell is shaded and the black dots show the Si trimers with the atomic structure in Fig. 1. (b) STM image of the square superstructure with diamond unit cell marked. Image size $197 \times 129 \text{ \AA}^2$. $V=+1.8$ V, $I=0.16$ nA.

TABLE I. Unit cell sizes observed for PTCDA on Ag/Si(111)- $\sqrt{3} \times \sqrt{3}$. The superstructures are given in matrix form as defined by Barlow and Raval (Ref. 25).

Phase	a (Å)	b (Å)	Area (Å ²)
$H-1$	12.4	19.6	243.0
$H-2$	12.23	19.16	234.3
Square	16.2	16.2	262.4
H second layer	12.4	19.8	245.5
H multilayer	12.1	20.1	243.2
α bulk	11.96	19.91	238.1
β bulk	19.30	12.45	240.3
Superstructure $H-1$	$\begin{pmatrix} 6 & 6 \\ -20 & -1 \end{pmatrix}$		
Superstructure square	$\begin{pmatrix} 15 & -9 \\ -9 & 15 \end{pmatrix}$		

The herringbone unit cell was found in two variations where the more frequent type ($H-1$) is shown in Fig. 2. This unit cell has size 12.4×19.6 Å², giving an area of 243.0 Å². The other unit cell size ($H-2$) is 12.23×19.16 Å² with an area of 234.3 Å². It is reasonable that there may exist other sizes of herringbone ordering as some were previously reported for PTCDA on substrates like Au(111) and Au(100).⁹ The $H-1$ and $H-2$ phases are not in agreement with the herringbone phase measured by Swarbrick *et al.* where a commensurate unit cell with the size 20.01×11.55 Å² was suggested.

In our STM data, the herringbone phase unit cell axes are very close to agree with high-symmetry directions of the $\sqrt{3} \times \sqrt{3}$ substrate, at least in most cases. Figure 2 shows an example of the herringbone phase ($H-1$) where the diagonal of the herringbone unit cell lies in the high-symmetry direction $[10\bar{1}]$ of the substrate. The short and long axes of the unit cell are close to the high-symmetry directions but still slightly off as seen on the extended lines following the substrate directions. In some images the herringbone structure appears with a lower degree of directional ordering, indicating that the substrate plays a smaller role in the ordering of this phase compared to the square phase. The fact that the unit cell size of the herringbone phase is very close to what is previously reported for the bulk phase is also an indication of this and suggests that the main cause of the herringbone ordering is the intermolecular forces.

Figure 5 shows a layer that has a mixture of the herringbone and square domains. In this case the interface is very sharp and in a high-symmetry direction of the substrate. It shows that the diagonal axis in the herringbone unit cell is parallel to the short axis of the square cell and lies in the $[01\bar{1}]$ direction. The diagonal appears to have a length of 2 times the distance between the molecular rows in the square phase. The unit cell of the square phase has already been determined, and this gives a good reference for the herringbone phase, which we assign as the second herringbone phase ($H-2$), with unit cell size of 12.23×19.16 Å².

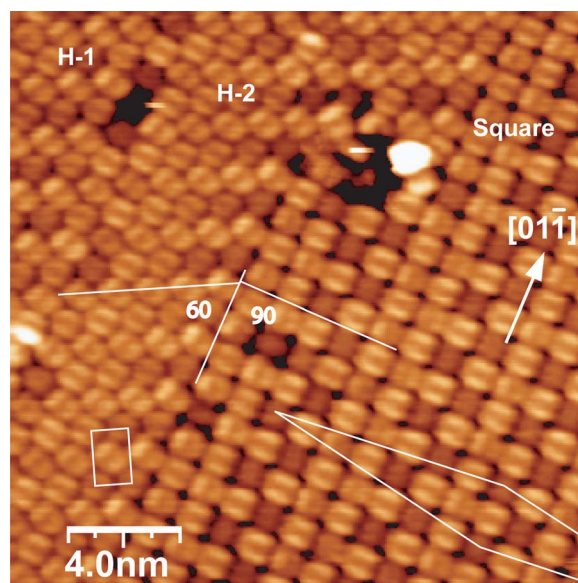


FIG. 5. (Color online) Molecular layer for 0.3 ML PTCDA deposition. The border between the square and herringbone phase can be seen. Areas with the $H-1$, $H-2$, and square phases, respectively, are seen. The diamond-shaped commensurate cell of the square phase is shown with molecules of equivalent adsorption sites at the corners. Image size is 200×200 Å², $V = -1.8$ V, $I = 0.5$ nA.

In some images, interesting superstructures, as observed in the square phase, are also seen for the $H-1$ phase. These modulations of the topograph indicate identical adsorption sites for molecules in the direction of the diagonal of the unit cell in the $[01\bar{1}]$ direction. An STM image with the herringbone unit cell and the smallest base for the surface modulations is shown in Fig. 6(a). A layer model of the relation with respect to the substrate is illustrated in Fig. 6(b). This model suggests that 6 units cells are needed to build up the superstructure, giving 12 different adsorption sites for the molecules. The unit cell in this model is 12.5×19.5 Å² in good agreement with the $H-1$ phase. In the above case the long and short axes of the herringbone unit cell are close to the

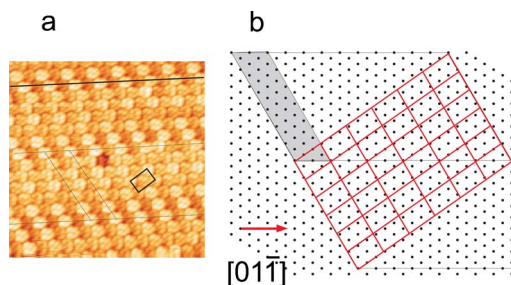


FIG. 6. (Color online) (a) Superstructure of the herringbone phase. The stripes are in the $[01\bar{1}]$ direction. The small rectangle is the herringbone unit cell. Image size is 200×200 Å², $V = -1.8$ V, $I = 0.104$ nA. (b) Model for the commensurate relation to the substrate. The black dots show $\sqrt{3} \times \sqrt{3}$ lattice points. The herringbone unit cell has one diagonal in the $[01\bar{1}]$ direction. The shaded commensurate superstructure contains 12 molecules with different adsorption sites.

high-symmetry directions of the substrate but only the diagonal is in complete agreement. The superstructure is clearly seen in filled-state STM images like Fig. 6(a) when using negative sample bias. As a matter of fact, the model in Fig. 6(b) also fits well with the herringbone structure in Fig. 2 in the diagonal direction of the unit cell (*C* line). The commensurate unit cell is shaded in Fig. 6(b) and has the size of $6 \times \sqrt{381}$ relative to the 1×1 lattice of the Si(111) surface, or $23.04 \times 74.95 \text{ \AA}^2$ with 12 molecules in the unit cell. The matrix notation of the unit cell is given in Table I.

Most of the herringbone domains were found with the basis axes in multiples of 60° in agreement with a sixfold symmetry. Three directions are from a threefold symmetry of the substrate, and in each of these directions there is a mirror plane giving a total of six symmetry directions. Inside the unit cell there is a clear electronic difference between these two molecules in the STM images. The sizes of the different PTCDA unit cells are listed in Table I and can be compared with the bulk α and β phases.⁴ It can be noted that the herringbone unit cells on the Ag/Si(111)- $\sqrt{3} \times \sqrt{3}$ surface generally are similar to the bulk phases. The square-phase unit cell occupies a larger area than the unit cell of the herringbone phases.

With an increased PTCDA coverage to 0.6 ML the growth of the molecular layer was quite similar to 0.3 ML but the domains are now larger. There was also a larger fraction of mixed islands even though the main part still has either the herringbone or square phase. There are, however, also herringbone structures with much lower directional ordering relative to the substrate. The unit cell size is still within error limits the same as for the *H*-1 phase. This suggests nonequilibrium growth where the mobility of the molecules is not high enough to form the herringbone phase in the more common, and possibly more energetically favorable, directions. Similar observations were previously reported for PTCDA on Au(111).⁹

At a coverage of one monolayer almost the whole surface was covered with a single layer of flat lying molecules. Both the herringbone and square phases could be observed. After careful analysis of various terraces and steps, we found that the growth of PTCDA follows a layer-by-layer mode; i.e., the first layer is filled before the second starts forming.

C. Two monolayers

At two-monolayer coverage the herringbone phase was dominating. The measured size of the unit cell was $19.8 \times 12.4 \text{ \AA}^2$ which is similar to the *H*-1 phase of the monolayer. There was no clear indication for more than one type of herringbonelike unit cell size in the second layer. In Fig. 7(a) a large area of the double layer can be seen. The areas with ordered structure are clearly divided by the step edges of the substrate but within the terrace there is a flat and almost defect-free top layer. The larger amount of defects at the step edges can here clearly be observed.

In previous STM studies of PTCDA only the herringbone phase has been reported for more than the first monolayer but here the square phase was still observed in the second monolayer as shown in Fig. 7(c). In this case the unit cell

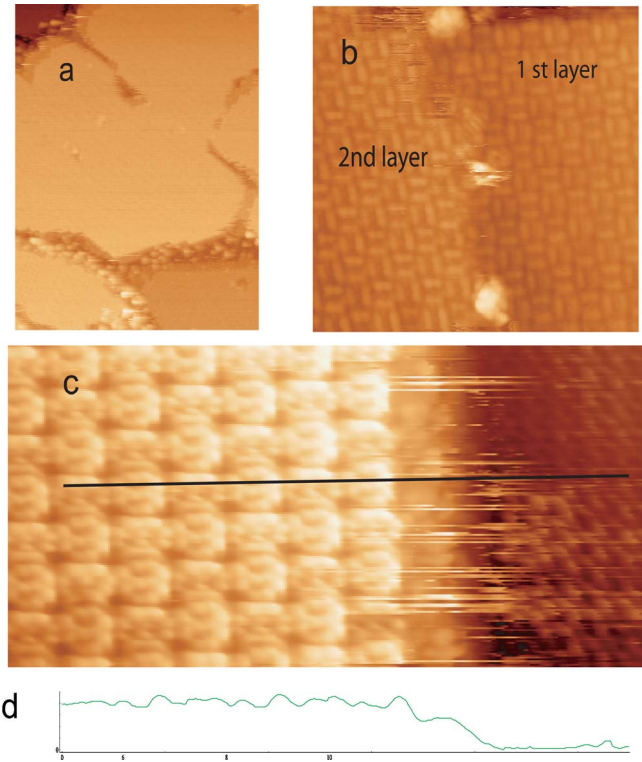


FIG. 7. (Color online) (a) 2 ML coverage of PTCDA. The image size is $600 \times 800 \text{ \AA}^2$. Measuring parameters images was $V = +2.52 \text{ V}$, $I = 50 \text{ pA}$. (b) Step between layers in the square phase. The image size is $150 \times 150 \text{ \AA}^2$. $V = +1.6 \text{ V}$, $I = 0.196 \text{ nA}$. (c) Double layer with square phase. The image size is $127 \times 64 \text{ \AA}^2$. Measuring parameters were $V = +1.8 \text{ V}$, $I = 0.240 \text{ nA}$. (d) Line profile recorded in (c).

size is clearly the same as the first monolayer but the rows are shifted by half the length of a molecule in the direction perpendicular to the step. In rare cases a slightly disturbed square phase was also observed as shown in Fig. 7(b). The angles of the unit cell in the top layer are not exactly 90° . This gives an almost square unit cell with slightly rotated orientation of the molecules. This suggests that the square phase is not stable at higher coverage.

D. Multilayers

The depositions of thicker films were done in two stages with nominal thicknesses of 5 and 10 ML. The substrate could not be observed above 2 ML deposition. The growth became more three dimensional with increasing thickness. On a larger scale, islands were formed but the islands clearly had a local layer structure with large flat terraces on top as seen in Fig. 8(a). Here, contrast variations seen at submonolayers were not observed. The observed unit cell sizes and symmetry directions in our measurements are quite similar over various islands and terraces. The typical top layer of a film has a unit cell of $20.0 \times 12.1 \text{ \AA}^2$, similar to the α bulk phase. For PTCDA coverages of more than two monolayers, the square phase was not observed. A layered structure of 10 ML PTCDA with typical island appearance is shown in Fig. 8(b). The layers are often terminated with sharp edges of

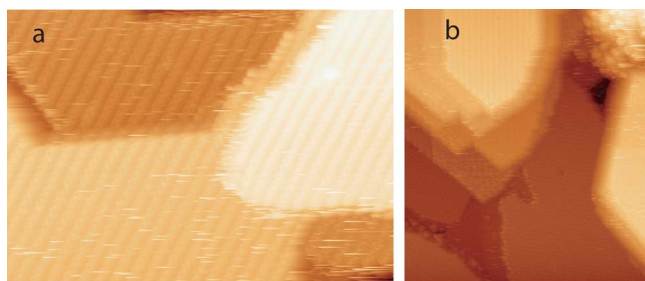


FIG. 8. (Color online) (a) Multilayer of PTCDA where direction and unit cell size for several layers on top of each other can be seen. The image size is $534 \times 375 \text{ \AA}^2$, $V = +2.46 \text{ V}$, $I = 17 \text{ pA}$. (b) Typical scan of the 10-ML-thick film. The image size is $800 \times 800 \text{ \AA}^2$, $V = +2.00 \text{ V}$, $I = 114 \text{ pA}$.

several monolayers high, but also with smaller terraces building up the whole structure. The top terraces for 5–10 ML are normally 50–100 nm in size.

IV. DISCUSSION

It is clear that the $\sqrt{3} \times \sqrt{3}$ surface is well suited for ordered growth of organic films as demonstrated both in this study and previous STM studies.^{15–21,26} A square and two herringbone phases have been observed at submonolayer coverage of PTCDA on the $\text{Ag}/\text{Si}(111)\text{-}\sqrt{3} \times \sqrt{3}$ surface. The herringbone phase is generally observed on weakly interacting substrates and in multilayers of PTCDA. The intermolecular force that gives this ordering is the local Coulombic attraction between the negatively charged O atoms in the carboxylic and anhydride groups and the positively charged H atoms in the perylene core.²⁷ It has been suggested, based on the distance between O and H-C that a hydrogen bond gives a further stabilization.²⁷ Calculations have shown that a square ordering is stable if the distance between equivalent molecules are 22.8 \AA .²³ This value is very close to the value $16.2 \times \sqrt{2} = 22.9 \text{ \AA}$ from our measurements on this surface. It was also suggested that the square phase is stabilized by hydrogen bonds.²³ It has previously been reported that when just molecular interactions are considered a square phase is less stable than a herringbone phase.²⁸ In our study, a square phase has clearly been observed from submonolayers and up to 2 ML but not for further growth. This means that a stabilizing interaction between the molecules and the $\text{Ag}/\text{Si}(111)\text{-}\sqrt{3} \times \sqrt{3}$ substrate occurs for the square phase.

Some adsorption positions for the square phase of PTCDA on the $\text{Ag}/\text{Si}(111)\text{-}\sqrt{3} \times \sqrt{3}$ substrate, based on the registry determined above [see Figs. 3 and 4(a)], are shown in detail in Fig. 9. Here, the substrate with Ag trimers, Si trimers, and PTCDA molecules is schematically illustrated. A model of a molecule with the long axis perpendicular to the $[01\bar{1}]$ direction is shown in Fig. 9(a). For this arrangement the perylene core of the molecule is positioned directly on top of one Si trimer. It can be noted that the carboxylic O atoms are close to Ag trimers. The molecules with their long axes parallel to the $[01\bar{1}]$ direction shown in Figs. 9(b) and 9(c), however, have a wider variation of positions relative to

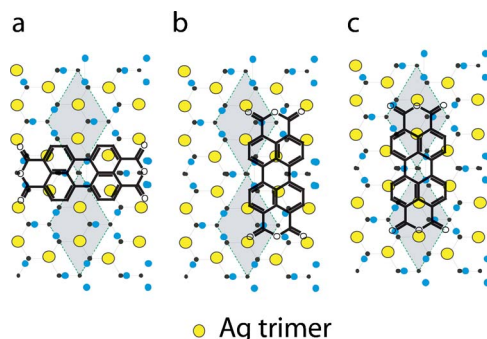


FIG. 9. (Color online) The $\text{Ag}/\text{Si}(111)\text{-}\sqrt{3} \times \sqrt{3}$ surface with the Ag and Si trimers and in scale PTCDA molecules. The large (yellow) circles show the center of an Ag trimer as seen in Fig. 1(b). (a) PTCDA molecule with the long axis perpendicular the $[01\bar{1}]$ direction centered over a Si trimer [corner molecule on the short axis in Fig. 4(a)]. (b) PTCDA molecule with the long axis parallel to the $[01\bar{1}]$ direction centered over two Ag trimers [third molecule from left in the middle row in Fig. 4(a)]. (c) PTCDA molecule with the long axis parallel to the $[01\bar{1}]$ direction centered over a Si trimer [middle molecule on the short axis in Fig. 4(a)].

the Ag trimers with two extreme cases: one where the center ring is above two Ag trimers and the perylene core is surrounded by the other four Ag trimers shown in Fig. 9(b) and another where the perylene core is centered over a Si trimer and surrounded by six Ag trimers. These two cases might account for maxima and minima in the STM intensity variations in this direction where the darker molecules have their center near a Si trimer and where the remaining configurations have an intensity in between.

The herringbone phase in the first layer has a unit cell similar to the bulk phases. This means that it is mainly due to the molecule-molecule interactions. A commensurate superstructure was seen for the *H*-1 phase. Another, smaller commensurate ordering in the herringbone phase was suggested by Swarbrick *et al.*²³ for PTCDA on $\text{Ag}/\text{Si}(111)\text{-}\sqrt{3} \times \sqrt{3}$ with a $3 \times 3\sqrt{3}(11.52 \times 19.95 \text{ \AA}^2)$ unit cell. This would give a long axis similar to the bulk phases but a shorter axis contracted by 4% from the α bulk phase. This implies that a stabilizing interaction is needed from the substrate. We did not observe this ordering and instead found larger unit cells. Possibly there could be some differences in growth conditions like temperature dependence that can activate the different adsorption mechanism. There is one case reported for PTCDA on (Ref. 1), where the formation of a commensurate herringbone phase was temperature dependent.

The mixture of the herringbone and square phases indicates a relatively high mobility of the molecules upon deposition. The coexistence also implies that the energies of the different phases are quite similar. The coexistence of the similar square and herringbone phases has also been found in the case of PTCDA on $\text{Au}(111)$ and $\text{Au}(100)$.⁹ The first five rows in the herringbone phase (*H*-2) next to the square phase border in Fig. 5 have a slightly smaller unit cell and also a slightly different modulation compared to the herringbone phase to the top left (*H*-1). This shows that the herringbone phase easily adjusts its structure to fit with the well defined adsorption points in the square phase.

The different positions relative to the Ag trimers could also account for the clear changes in the XPS O 1s and C 1s spectra in our recent photoelectron spectroscopy (PES) study of PTCDA on Ag/Si(111)- $\sqrt{3} \times \sqrt{3}$.²² A gradual change in the XPS spectra when film thickness increased from submonolayer to higher coverage was seen. At low coverage new components in the O 1s and C 1s spectra were present, which were not previously observed for PTCDA on weakly interacting substrates. Also the highest occupied and lowest unoccupied molecular orbitals (HOMO and LUMO) levels were found to be modified at monolayer coverage, indicating that the entire molecules are affected by the interaction between molecules and substrate.

Experimental methods like PES integrate the signal over a large area covering all molecular configurations, so it is hard to compare these results and assign new components to specific interactions on a single molecule. The LEED pattern observed in our previous study²² where several coexisting phases were indicated is in agreement with the STM results; i.e., the LEED pattern is consistent with a mixture of herringbone and square phases.

At high coverage PTCDA appears to grow in the α bulk phase with a layer-by-layer mode. The multilayer structures seem to be separated by the substrate step edges. The size of the top layer is generally in the same range as the substrate terraces of the clean Ag/Si(111)- $\sqrt{3} \times \sqrt{3}$ substrate. This suggests that larger defect-free terraces in the substrate can promote larger multilayer terraces.

V. CONCLUSIONS

PTCDA has been grown on Ag/Si(111)- $\sqrt{3} \times \sqrt{3}$, and two different commensurate phases have been found in the submonolayer range: a square and a herringbone phase. The commensurate superstructure of the square phase has a diamond-shaped unit cell containing 14 molecules. Adsorption sites on top of the $\sqrt{3} \times \sqrt{3}$ substrate have been determined. The other phase is a herringbone structure with two molecules in the unit cell. This growth mode is more compact and to a higher degree governed by the intermolecular forces. The unit cells in the herringbone phase at monolayer coverage are similar to the ones found in bulk α and β polymorph. The $H-1$ phase has a commensurate relation to the substrate with the diagonal of the unit cell in the $[01\bar{1}]$ direction. The herringbone phase has also been found with a second unit cell size ($H-2$) and in some cases with a lower ordering relative to the substrate. Both the square and herringbone phases are observed in the second layer with unit cells of the similar size as in the first layer. For more than two monolayers only the herringbone phase is stable and the growth is similar to the α polymorph. The thicker layers grow in a layer-by-layer mode limited in size mainly by the steps in the substrate.

ACKNOWLEDGMENT

The work done here was funded by the Swedish Research Council.

*Electronic address: jorgen.gustafsson@kau.se

- ¹M. Eremtchenko, J. A. Schaefer, and F. S. Tautz, *Nature (London)* **425**, 602 (2003).
- ²M. Stöhr, M. Gabriel, and R. Möller, *Surf. Sci.* **507-510**, 330 (2002).
- ³C. Seidel, C. Awater, X. D. Liu, R. Ellerbrake, and H. Fuchs, *Surf. Sci.* **371**, 123 (1997).
- ⁴S. R. Forrest, *Chem. Rev. (Washington, D.C.)* **97**, 1793 (1997).
- ⁵Y. Hirose, S. R. Forrest, and A. Kahn, *Phys. Rev. B* **52**, 14040 (1995).
- ⁶J. B. Gustafsson, E. Moons, S. M. Widstrand, and L. S. O. Johansson, *Surf. Sci.* **572**, 23 (2004).
- ⁷E. Umbach, K. Glöcker, and M. Sokolowski, *Surf. Sci.* **402-404**, 20 (2002).
- ⁸A. Kraft, R. Temirov, S. K. M. Henze, S. Soubatch, M. Rohlfing, and F. S. Tautz, *Phys. Rev. B* **74**, 041402(R) (2006).
- ⁹S. Mannsfeld, M. Törker, T. Schmitz-Hübsch, F. Sellam, T. Fritz, and K. Leo, *Org. Electron.* **2**, 121 (2001).
- ¹⁰T. Soubiron, V. Vaurette, J. P. Nys, B. Grandidier, X. Wallart, and S. Stiévenard, *Surf. Sci.* **581**, 178 (2005).
- ¹¹E. Umbach, M. Sokolowski, and R. Fink, *Appl. Phys. A: Mater. Sci. Process.* **63**, 565 (1996).
- ¹²R. I. G. Uhrberg, H. M. Zhang, T. Balasubramanian, E. Landemark, and H. W. Yeom, *Phys. Rev. B* **65**, 081305(R) (2002).
- ¹³N. Sato, T. Nagao, and S. Hasegawa, *Surf. Sci.* **442**, 65 (1999).
- ¹⁴H. M. Zhang, J. B. Gustafsson, and L. S. O. Johansson, *Phys. Rev. B* **74**, 201304(R) (2006).
- ¹⁵P. Guaino, D. Carty, G. Hughes, P. Moriarty, and A. A. Cafolla,

Appl. Surf. Sci. **212-213**, 537 (2003).

- ¹⁶M. D. Upward, P. Moriarty, and P. H. Beton, *Phys. Rev. B* **56**, R1704 (1997).
- ¹⁷T. Nakayama, J. Onoe, K. Takeuchi, and M. Aono, *Phys. Rev. B* **59**, 12627 (1999).
- ¹⁸M. D. Upward, P. H. Beton, and P. Moriarty, *Surf. Sci.* **441**, 21 (1999).
- ¹⁹M. J. Butcher, J. W. Nolan, M. R. C. Hunt, P. H. Beton, L. Dunsch, P. Kuran, P. Geiorgi, and T. J. S. Dennis, *Phys. Rev. B* **64**, 195401 (2001).
- ²⁰D. L. Keeling, N. S. Oxtoby, C. Wilson, M. J. Humphry, N. R. Champness, and P. H. Beton, *Nano Lett.* **3**, 9 (2002).
- ²¹J. A. Theobald, N. S. Oxtoby, M. A. Philips, N. R. Champness, and P. H. Beton, *Nature (London)* **424**, 1029 (2003).
- ²²J. B. Gustafsson, H. M. Zhang, E. Moons, and L. S. O. Johansson, preceding paper, *Phys. Rev. B* **75**, 155413 (2007).
- ²³J. C. Swarbrick, J. Ma, J. A. Theobald, N. S. Oxtoby, J. N. O'Shea, N. R. Champness, and P. H. Beton, *J. Phys. Chem. B* **109**, 12167 (2005).
- ²⁴A. Ishizaka and Y. Shiraki, *J. Electrochem. Soc.* **133**, 666 (1986).
- ²⁵S. Barlow and R. Raval, *Surf. Sci. Rep.* **50**, 201 (2003).
- ²⁶P. Guaino, A. A. Cafolla, D. Carty, G. Sheerin, and G. Hughes, *Surf. Sci.* **540**, 107 (2003).
- ²⁷Q. Chen, T. Rada, T. Bitzer, and N. Richardson, *Surf. Sci.* **547**, 385 (2003).
- ²⁸R. Staub, M. Toerker, T. Fritz, T. Schmitz-Hübsch, F. Sellam, and K. Leo, *Surf. Sci.* **445**, 368 (2000).